Available online www.jsaer.com

***Journal of Scientific and Engineering Research*, 2020, 7(1):235-245**

Research Article

ISSN: 2394-2630
CODEN(USA): JSERBR

Geotechnical Analysis for Crossing Tunnels in Sand Soil

Mohamed Saied Abd El-Samie El-bahrawy

Department of Geotechnical Civil Engineering, Faculty of Shoubra Engineering, Benha University, Egypt

Abstract Currently, the development of underground construction, multi-tunnel engineering has become a matter of concern since the interaction between tunnels at close ranges could cause additional deformation in surrounding structures and even serious damage to surface buildings.

These tunnel displacement and soil deformation can be predicted using numerical methods considering the influence of various factors, such as the nature of sand soil. The elasto-plastic constitutive model is implemented in finite element to investigate deformation problems in the strata and nearby structures caused by the excavation of multi-tunnels.

This paper focuses on configurations of two crossing tunnels. Multiple 3Dnumerical simulations using ansys enable successive analyses conducted for tunnels at different spacings (1.5D, 2.5D, 3.5D and4.5D, where D is the tunnel diameter) of configurations vertically.

The results, including the ground settlement and tunnel convergence, are analyzed. For each results, the most unfavorable case is determined by comparing the resultsof different cases. This investigation can provide a reference for multi-tunnels design and construction.

Keywords Multi-tunnels, Sand, Ground loss, Finite element, Constitutive relation

1. Introduction

With the development of the land utilization rate in large cities, creating interest in the development of underground space, followed by the construction of subways, underground passages, urban pipe corridors and so on.

However, underground space is limited. To maximize the use of underground space, multi-structure intersections have become increasingly common. In recent years, the development of underground space has been planned in cities such as Beijing, Shanghai and Nanjing [1-2]. However, there are already many existing underground structures, such as pile foundations, municipal pipelines and tunnels, which may hinder the development of three-dimensional underground space use.

Therefore, new tunnel construction often needs to bypass existing structures with a parallel or cross configuration [3]. In addition, the construction of new underground structures affects the normal operation of ground surface structures.

Thus, complex crossing tunnels have potential construction risks and safety hazards and adversely affect adjacent structures (e.g., by inducing building cracks or exceeding the bearing capacity of operating tunnels) [4]. This limitation is especially obvious in sand soil. Therefore, it is necessary to fully understand the land subsidence caused by the construction of crossing tunnels and the impact on existing adjacent tunnels.

It is generally believed that the impact of newly built tunnels on existing tunnels is due to the disturbance of the internal forces of the tunnel structure caused by soil disturbances. At present, there are mainly three methods for studying the multiline crossing of tunnels: (1) empirical or field measurement methods, (2) the model test method, and (3) the numerical analysis method. Based on the field survey data, empirical methods as

implemented in a previous study were used to calculate the change of the internal force of the tunnel lining caused by surface settlement and adjacent construction [5-6].

It is clear that field observations remain the key to understanding the interaction between adjacent tunnels. Unfortunately, field data are often incomplete. The structural forces induced in tunnel linings are thus hard to obtain. The empirical and analysis method, using the superposition method [7], is based on the prediction of each tunnel's individual excavation, and the final settlement curve is obtained by superposition. In general, the superposition method cannot rigorously consider the effect of an existing tunnel or the repeated unloading of the ground caused by the previous excavation of the first tunnel; therefore, the settlement curves do not predict the final displacement very well [8].

Model tests, in particular the centrifuge model test, are another preferred choice for the study of underground works since the same stress state in the tests is used to simulate the actual stress state of the soil [9]. However, the model test study is difficult to implement for large-scale tests. Furthermore, the cost of the model test is high, which limits its application. Recently, the discrete element method was also used to simulate tunnel excavation [10] but only for a small scale with a very limited number of soil particles.

Numerical analysis, as a convenient and effective search tool, has been widely used by researchers and engineers [11-13]. As far as multi-tunnel excavation is concerned, the introduction of appropriate boundary conditions and appropriate constitutive models [3] makes it possible to predict land subsidence using numerical analysis methods. Here, the constitutive model of the soil plays an important role. In previous studies, a variety of soil constitutive models were used to analyze problems such as ground settlement caused by tunnel openings, such as nonlinear elastic models with transverse anisotropy [14], the Mohr–Coulomb model [15], the double surface soil hardening model [16] and the hypoplastic model [17]. However, most models are more or less limited in the simulation of the mechanical properties of sand soil;

This paper focuses on the three-dimensional cross excavation problem of two tunnels. The numerical analysis method is used to study the effect of multi-tunnel excavation on the settlement of the ground surface and the effect on the first tunnel induced by the second tunnel from two aspects: the relative position of the tunnels and the distance between them. A series of three-dimensional finite element models were constructed to consider the intersection of two tunnels with different relative positions and different spacings. In order to consider the influence of soil an isotropy on the excavation problem, the Mohr–Coulomb model was introduced as a user-defined material into the finite element code. Through the above calculations, the analysis of ground settlement caused by the excavation of the crossing tunnels, the change of tunnel internal forces and the convergence of the first tunnel are analyzed and summarized.

2. Numerical Models

As described by Divall and Goodey [8], eight-group plane twin-tunnel centrifuge model tests were conducted to investigate the ground deformation as affected by twin tunnel excavation. The size of the centrifuge tank is 500 mm _ 200 mm _ 180 mm, and the radius of the tunnelis 40 mm. The applied acceleration is 100g, where g is the gravitational acceleration. The 2D FEM simulation on investigating the ground deformation affected by twin tunnel excavation has been validated by comparing simulated results and measured data. In this study, the 2D simulation is extended to 3D simulation for a more comprehensive understanding of the ground deformation affected by multi-tunnel excavation. Thus, a series of three-dimensional finite element simulation models of crossing tunnels is presented. These models take into account the ground volume loss via nonuniform contraction methods. However, only simulated results are presented to show the evolution of volume loss-induced ground deformation because there are no available data under 3D conditions.

2.1. Simulation program

In order to study the soil response caused by the excavation of crossing tunnels and the effects of tunnels on each other, this paper designs a numerical model test for crossing tunnels with 8 different tunnel relative positions and tunnel spacing's (see Figs. 1(a) and (b)). In order to reduce the response of the initial state to the first-excavated tunnel caused by tunneling, the location of this first tunnel is fixed. The tunnel diameter D = 4 m is determined according to the centrifuge model test under 100g [8]. The lining is assumed to have zero

thickness. The tunnel spacing ranges from 1.5D to 4.5D (both upper and lower sides), where D is the tunnel diameter.

2.2 Finite element models

All numerical models in this paper are consistent in size to reduce size effects. In addition, in order to control the boundary effect and reduce the amount of calculation at the same time, according to the recommendations for finite element calculations such as those of Mo¨ ller [12], the appropriate boundary conditions are selected based on the distance between tunnels. The largest boundary of the model is determined by the maximum spacing of the tunnel, which is 4.5D (case 8) in this study (Fig. 1). The horizontal displacements of the four vertical boundaries of the model sides are fixed, allowing only vertical displacements. The bottom boundary of the model is completely fixed in both the horizontal and vertical directions. The finite element model extends in the depth direction to a minimum depth of four times the tunnel diameter. The width, depth, and length of the final model are all 15D, and the model boundaries extend laterally along the tunnel axis to be greater than 5D and longitudinally along the tunnel extending beyond 15D.

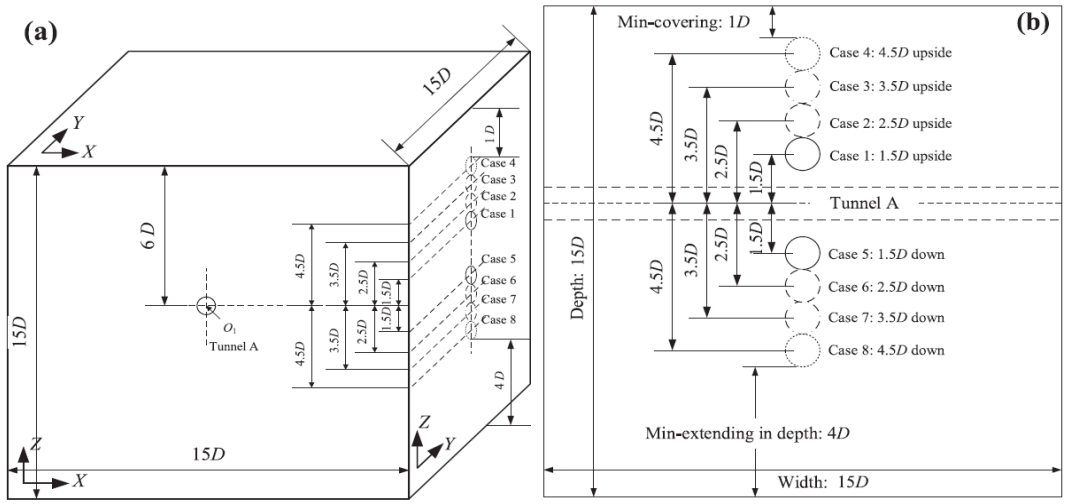

Figure 1: Cases of the crossing tunnel model: (a) 3D view, and (b) cross-section view

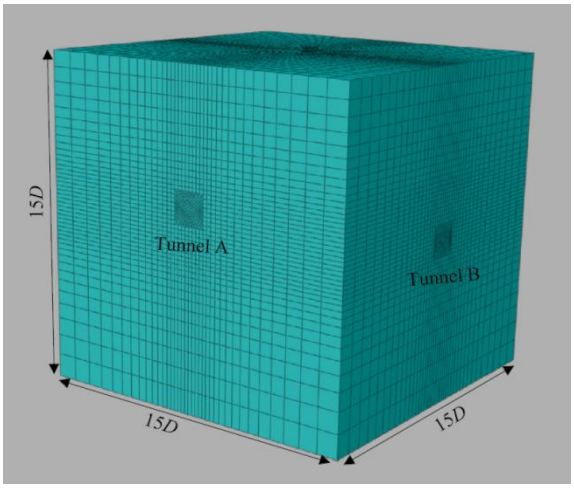

Figure 2: The meshed finite element model

Tunnel A is the first tunnel, and tunnel B is the second tunnel. Effective stress is used in the finite element analysis. The variation of soil modulus (Es) with confining pressure is related to effective pressure based on Janbu's empirical equation as presented in Eq. (1). The different soil parameters (m, n) are selected to simulate the behavior of sand soil.

$$E_s = mP_a\left(\frac{\sigma_3}{P_a}\right)^n \quad (1)$$

In which, modulus number (m) and exponent number (n)are both pure numbers, Pa is the Fig. 2. Meshed finite element model. Atmospheric pressure expressed in appropriate units, and σ3 is an effective confining pressure.

Geotechnical properties	**Sand soil**
Bulk density (t/m^3)	1.95
Poisson's ratio	0.30
Effective angle of initial friction	38
Effective cohesion, C(t/m2)	0
Standard penetration (blows/0.3 m)	32
Modulus number (m)	600
Exponent number (n)	0.52
Over consolidation ratio (OCR)	–
Coefficient of lateral earth pressure, K0	0.385

Type	**E_b (t/m^2)**	**F_c (t/m^2)**	**γ (t/m^3)**	**Poisson's ratio**
Tunnel liner	2.1 * 10^6	4000	2.5	0.20

2.4. Modeling of over excavation

Excavation is considered to be one of the main causes of the loss of foundation soil. In tunnel shield construction, the difference between the diameter of the cutter head and the shield machine in the shield tunneling process is one of the main reasons for over excavation. Other factors, such as turning during shield driving, can also lead to over exploitation of foundation soils. In general, the loss of soil caused by over excavation is strictly controlled by grouting and other methods in the construction of shield tunnels. Considering various factors, the maximum volume loss in this study is 3%, corresponding to a previous model test [8].

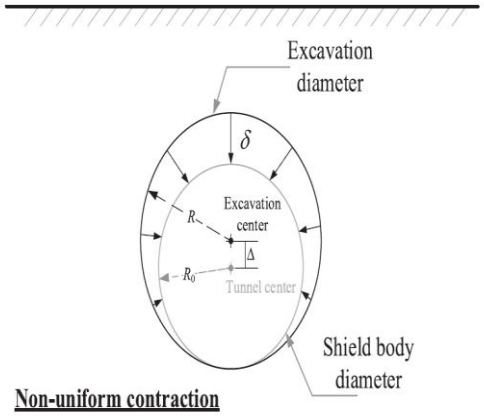

Figure 3: Nonuniform ground contraction

In the finite element analysis, there are two typical shrinkage models for the modeling of foundation soil loss: uniform shrinkage and nonuniform shrinkage [18]. In this study, the nonuniform distribution of the strata loss simulation method was adopted, as shown in Fig. 3. Although this loss model is more complex, it is more consistent with the actual project. In this simulation method, the maximum ground displacement (i.e., δ in Fig. 3) appears at the top of the tunnel, and the ''shrinking center" coincides with the center of the tunnel, where Δ is the distance between the excavation center and the center of the tunnel.

2.5. Modeling of tunnel excavation

The excavation and construction of the tunnel were simulated in a step-by-step procedure, incorporating the ''element death" approach, which is widely employed in finite element analysis of excavation problems [19]. The whole modeling process is shown in Fig. 4:

(i) In the first phase, the initial stress field is assigned based on the geostatic equilibrium achieved, ensuring that the corresponding deformations are not taken into account in further steps.

(ii) In the second step, the first tunnel (tunnel A) is excavated by deactivating the corresponding excavation volume elements. In addition, the excavation boundary of the over excavated tunnel ring is fixed, shown in Fig. 5(a).
(iii) Thereafter, nonuniformly distributed displacement boundaries are applied on soil nodes in the perimeter of the excavation space to account for the volume loss, shown in Fig. 5(b).
(iv) The tunnel lining of tunnel A is added. The excavation of tunnel A is completed.
(v), (vi), and (vii) are the steps of excavation for tunnel B, which likely repeats the three steps above.

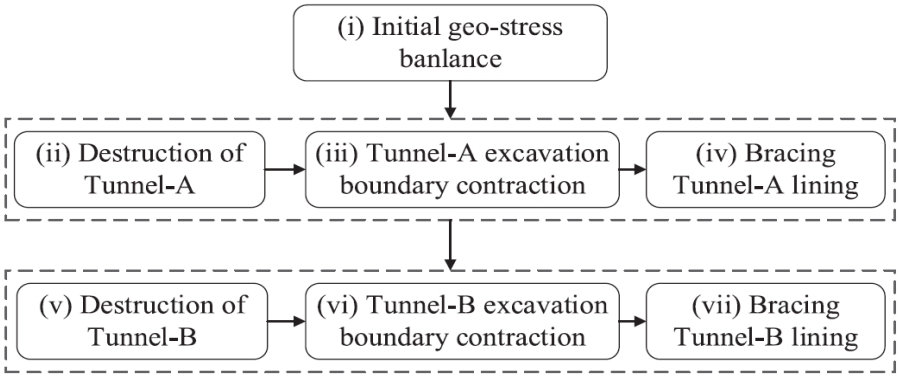

Figure 4: Numerical simulation steps for tunneling excavation

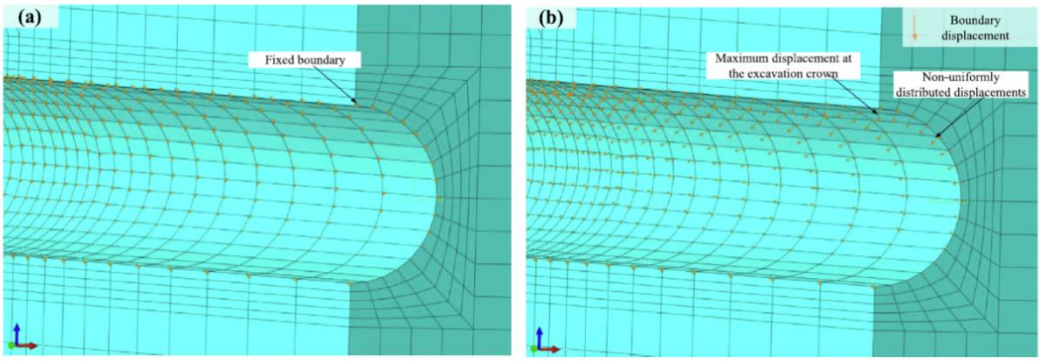

Figure 5: (a) meshed model of fixed excavation boundary and (b) mesh model of nonuniform displacement

3. Simulation results

In this study, the ground settlement caused by the excavation of crossing tunnels is studied through calculation and analysis. The axial force, bending moment, tunnel displacement and diameter convergence of tunnel linings are first evaluated.

3.1. Ground settlement

Figure 6 presents the final settlement of the soil after excavation is completed when the 2nd tunnel is constructed above the existing tunnel with different tunnel spacings. As seen from the figure, the settlement of the soil is approximately symmetrical about the tunnel axis, and the maximum vertical displacement occurs near the axis of the tunnel. For the first excavation of tunnel A, the soil at the bottom of the tunnel produces a bulge, which is caused by the unloading of the bottom soil caused by the tunnel excavation. In addition, as the distance between tunnels increases, the settlement of the soil shrinks, and the range of bulging increases.

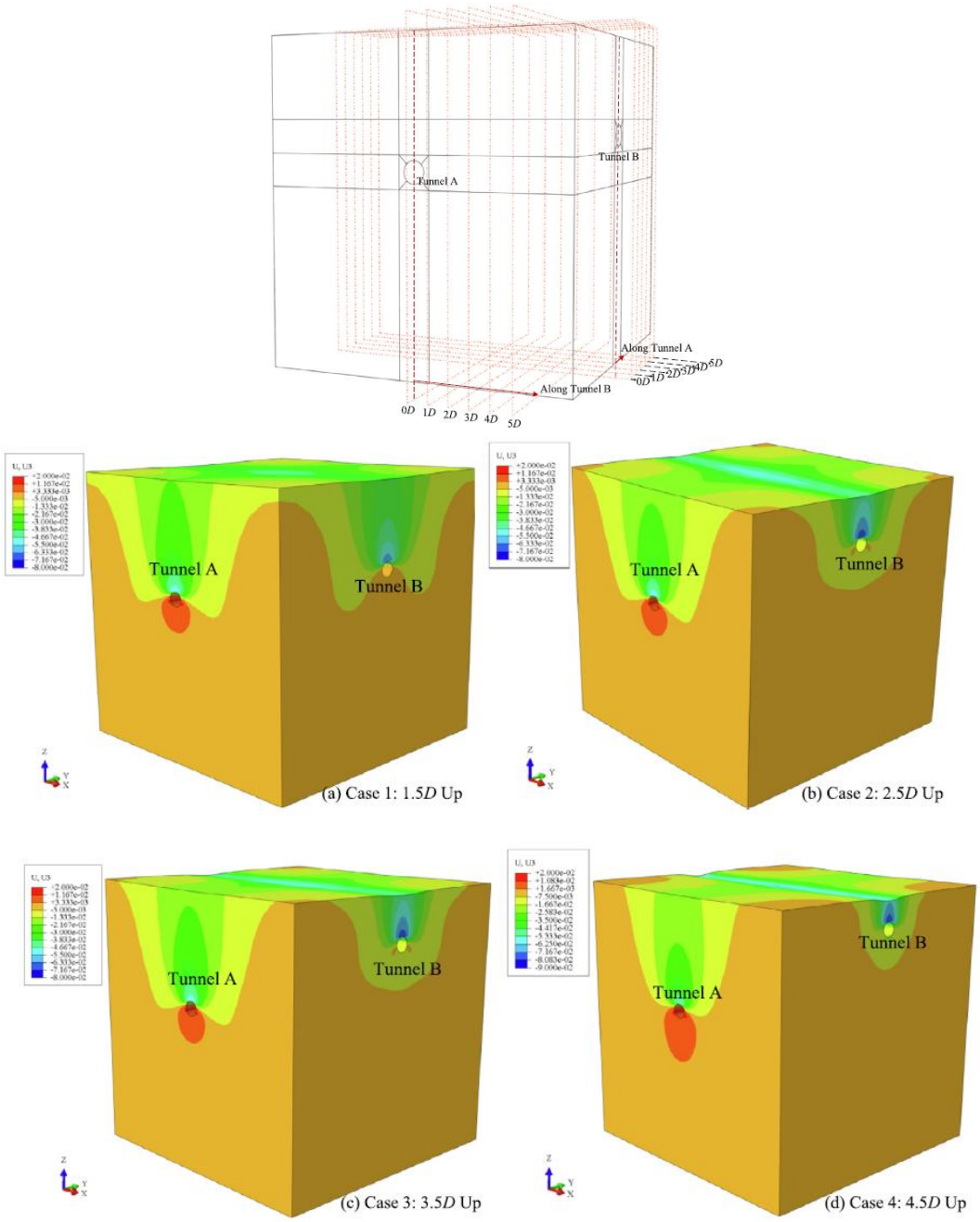

Figure 6: Vertical displacements for the cases where tunnel B is above tunnel A: (a) case 1, (b) case 2, (c) case 3, and (d) case 4

Figure 7 presents the settlement of tunnel B constructed after tunnel A at different tunnel spacings. Similar to the previous cases, the overall settlement is distributed symmetrically along the axis of the tunnel, and the soil at the bottom of the tunnel is bulging. However, the difference is that as the distance between the tunnels increases, the range of soil uplift in the tunnel decreases, indicating that when the depth of the tunnel is greater, the bulging effect due to stress release decreases.

To further analyze the land subsidence caused by tunnel excavation, cut the section perpendicular to the axis of the tunnel along the longitudinal direction of the two tunnels (see Fig. 8), and plot the surface settlement of the section. The sections taken are divided into two groups according to the section of the tunnel axis, i.e., longitudinal settlement along tunnel A and longitudinal settlement along tunnel B. Six sections are selected in each direction, spaced 1D apart, extending outward from the center of the tunnel. The surface subsidence of the

section taken will be analyzed and discussed separately in the following sections. Fig. 8. Vertical sections selected along both tunnels.

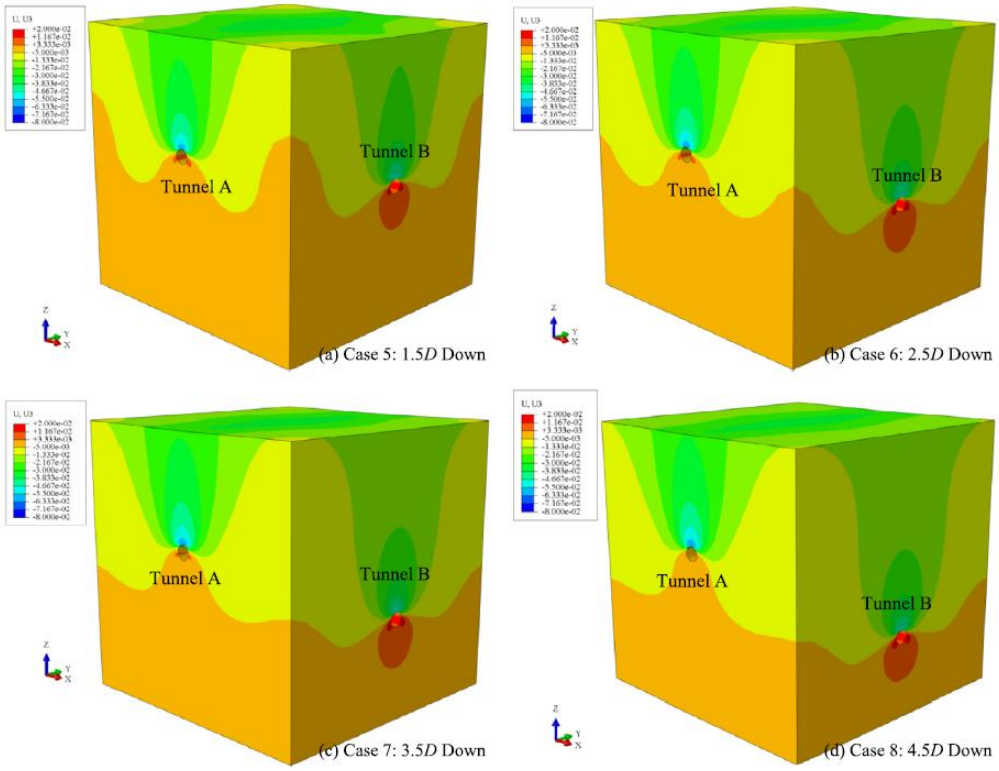

Figure 7: Vertical displacements for the cases where tunnel B is below tunnel A: (a) case 5, (b) case 6, (c) case 7, and (d) case 8

3.2. Ground settlement along the longitudinal direction of tunnel A

Figure 9 shows the final surface settlement along the longitudinal direction of tunnel A when tunnel B passes under tunnel A at different spacings. When tunnel B passes below tunnel A, the surface settlement caused by the change in tunnel spacing changes by a smaller amount.

Comparing these four cases, the maximum settlement is close to 0.03 m, and the difference in maximum settlement between different cases is very slight. Each case has surface settlement decreasing with increasing distance from the center of the model.

The maximum settlement in all cases in which tunnel B passes below tunnel A occurs in the center of the model as well as the center of the tunnel (indicated by the red line in the figure). The blue line in the figure is the 0D section settlement curve caused by tunnel A being excavated alone. A comparison of the settlement curves, the red line and blue line, indicates that the maximum settlement after completion of the construction is less than twice the settlement caused by tunnel A excavation.

Figure 10 shows the ground settlement along the longitudinal section of tunnel A when the back-excavated tunnel (tunnel B) is crossed from above. As seen from the figure, the maximum settlement also occurs near the location of the tunnel axis.

The maximum settlement at the surface of the tunnel increases with increasing tunnel spacing. The shallower the tunnel is, the more important the ground surface settlement. The maximum settlement is increased from 0.04 m to 0.62 mm when the tunnel spacing increases from 1.5D to 4.5D.

The blue line in the figure is the settlement curve of the 0D section when tunnel A is excavated alone, and the red line is the settlement curve of the 0D section after completion of the excavation of the two tunnels. Comparing the two curves, it can be seen that the settlement after the final excavation of the tunnels is more than twice as large as that of the excavation of tunnel A. When the tunnel spacing is 4.5D, the final settlement exceeds 3times the settlement caused by excavation of just one tunnel. Similar to the case of the tunnel exposed

to operating conditions, the farther away from the central axis of the tunnel, the shallower the settlement curve is, that is, the smaller the settlement.

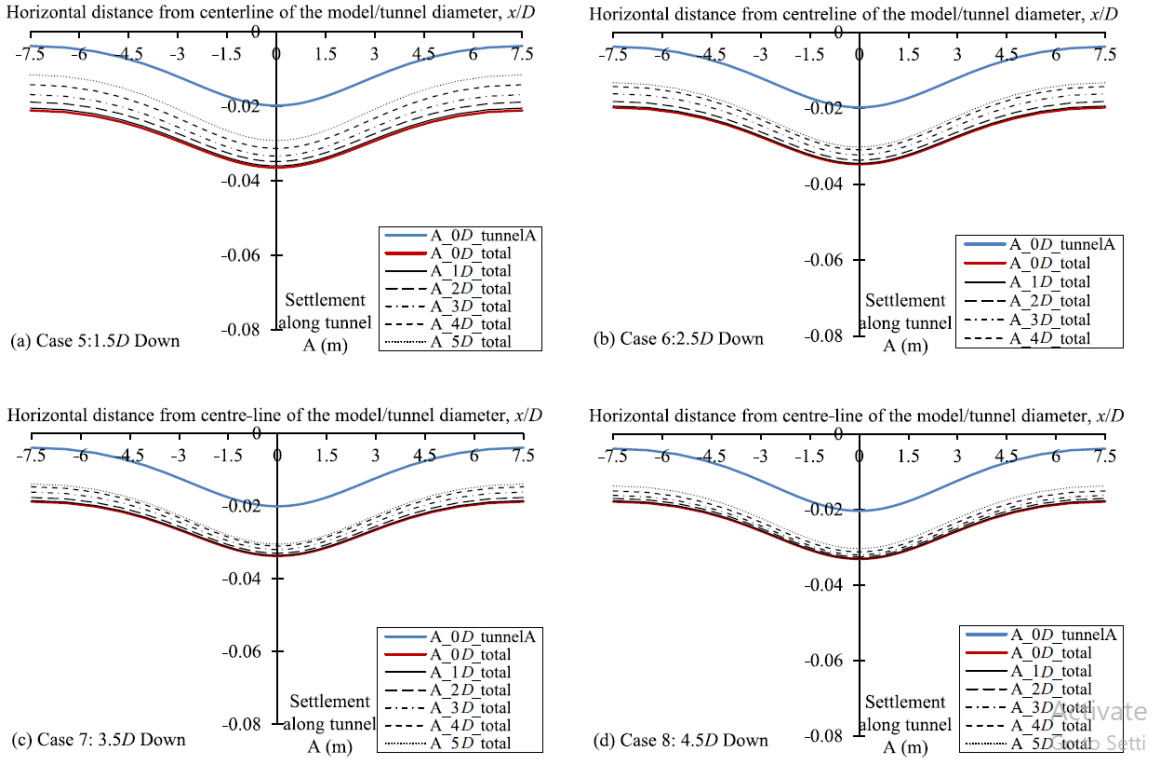

Figure 9: Final settl. along tunnel A for the cases where tunnel B is below tunnel A: (a) case 5, (b) case 6, (c) case 7, and (d) case 8

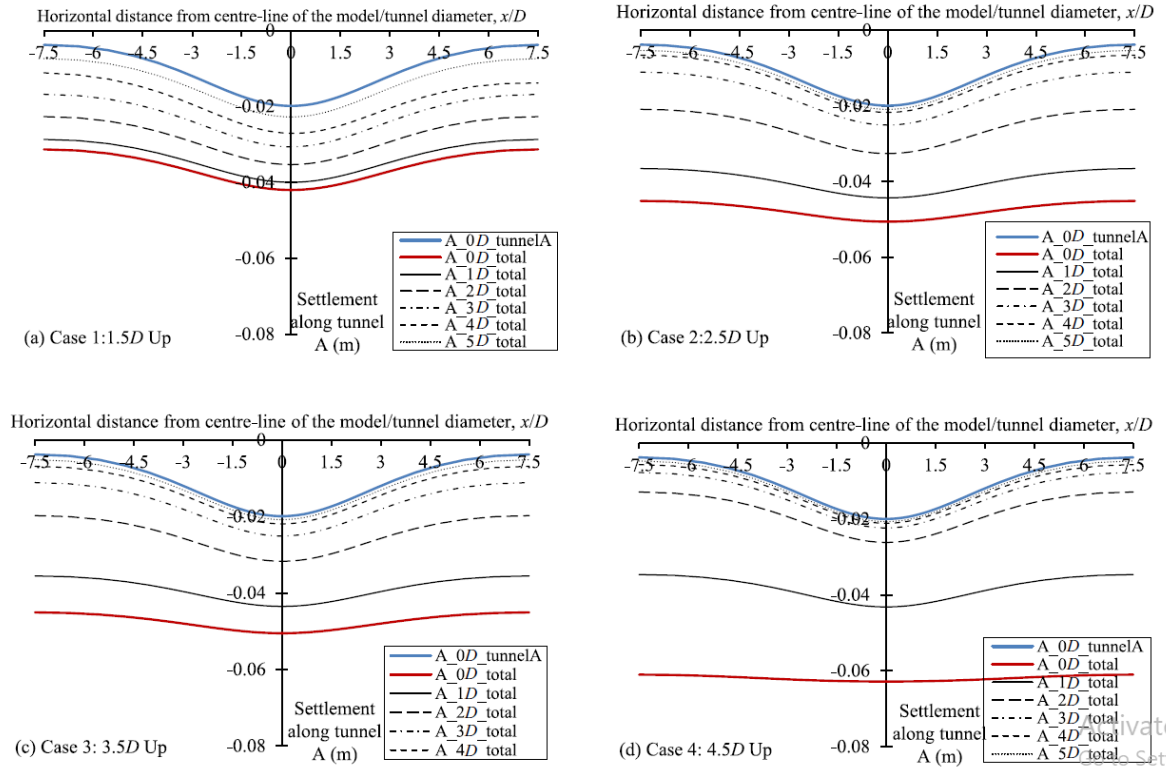

Figure 10: Final settl. along tunnel A for cases where tunnel B is above tunnel A: (a) case 1, (b) case 2, (c) case 3, and (d) case 4

Note that the range of the influence zone due to tunnel excavation is significantly affected by the soil model used. In this case, the Mohr–Coulomb model does not incorporate the small-strain stiffness, so the ground surface settlements at the two ends of the FEM model are too large, and the influence zone of ground surface settlement is too wide. To accurately predict the influence zone of ground surface settlement, a more advanced soil model considering the small-strain stiffness should be adopted.

To further investigate the ground settlement caused by tunnel excavation of another tunnel, the parameter DSmax was used to study the settlement caused by tunneling. This parameter can be described by Eq. (9). The physical meaning of this value is the ratio of the settlement caused by the excavation of the tunnel after excavation (tunnel B) alone to the settlement caused by the first tunnel (tunnel A).

$$\Delta S_{max} = \frac{S_{max,f} - S_{max,A}}{S_{max,A}} \quad (2)$$

Where $S_{max,f}$ is the maximum settlement of the final settlement of each section and $S_{max,A}$ is the maximum tunnel A settlement.

Figure 11 presents a graph of DSmax for different sections. The coordinate is DSmax, and the abscissa is the position of the corresponding section. The maximum value of DSmax is greater than that of the condition of crossing below in all the simulation cases when tunnel B is crossing above, while the minimum value of DSmax is less than that of the condition of crossing below. At the same time, for all operating conditions, the settlement gradually decreases as the distance from the crossing center increases. This result shows that the tunnel has an obvious influence on surface settlement when it passes through the existing tunnel, but it has a smaller impact on the surface. The shallower the buried depth of the tunnel, the more pronounced is the change in the DSmax distance at the center of the tunnel. The maximum value of DSmax is 2.16, which occurs in the 4.5D condition (in the case where tunnel B is 4.5D above tunnel A), indicating that the maximum settlement caused by tunnel B is twice the settlement caused by tunnel A of this case, 1 time more than that of the other cases.

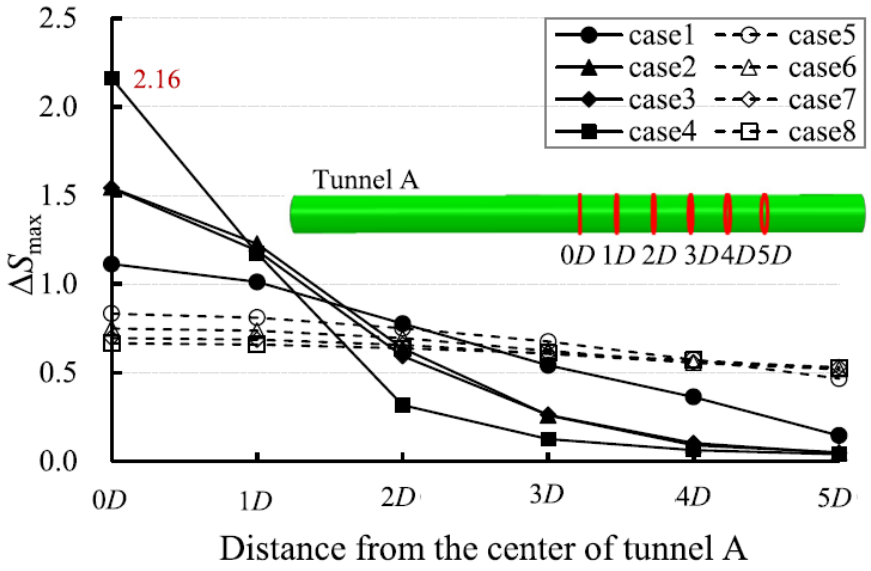

Figure 11: ΔS_{max} along the tunnel A direction in different cases

3.3. Convergence of tunnel A

Tunnel convergence is a widely used parameter to measure the deformation of a tunnel [20]. The convergence can be defined as shown in Fig. 12.

Figure 13 presents some typical sections selected to plot the maximum convergence of tunnel A caused by tunnel B excavation. The maximum convergence of tunnel A is 0.27‰, which occurs in tunnel B passing less than 1.5 Dunder tunnel A (case 5). Tunnel A as affected by tunnel B excavation exhibits greater deformation. When the impact received at the center of the axial force bending tunnel is the largest, for convergence deformation, the convergence occurs at a position deviating from the center of the tunnel. The convergence

amount increases from 0D to 3Dfrom the center of the tunnel and decreases when the distance is greater than 3D.

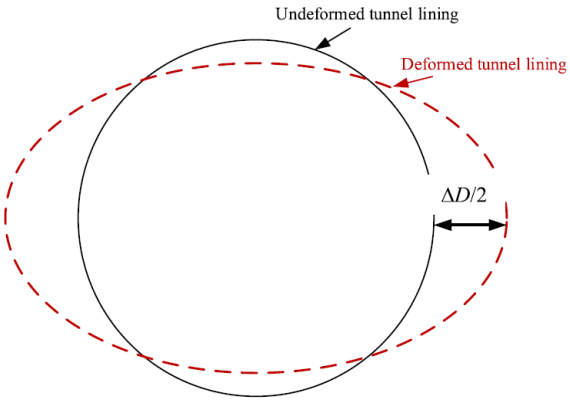

Figure 12: Definition of the convergence

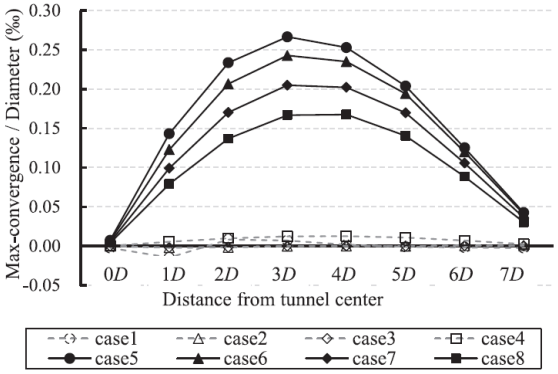

Figure 13: Convergence/diameter against the distance from the tunnel center

4. Conclusions

This study analyzes the problems caused by tunnel excavation under different three-dimensional intersections of two crossing tunnels with different spacings in a sand foundation. The elasto-plastic constitutive model. A yielding function of the Mohr–Coulomb types and a plastic function of the Drucker–Prager type are adopted in this study. Based on model tests and actual engineering conditions, a finite element model of eight crossing tunnels with different tunnel spacings (from 1.5D to 4.5D) was established.

Based on numerical simulation results, the ground settlement, and tunnel displacement caused by tunnel excavation under different conditions were analyzed, and the following two conclusions were obtained:

(1) The ground settlement is symmetrical along the axis of the tunnel, and the maximum settlement of the surface is generated at the location of the tunnel axis. The ground settlement caused by the excavation of two crossing tunnels when the second tunnel is excavated above the first tunnel is greater than the settlement when the second tunnel is excavated below the first tunnel. The shallower the buried tunnel is, the larger the maximum settlement on the surface is and the narrower the shape of the settlement is. At the same time, the maximum settlement caused by the excavation of crossing tunnels when the second tunnel is excavated above the first tunnel is more than twice that caused by the excavation of the first tunnel.

However, the maximum settlement caused by the excavation of crossing tunnels when the second tunnel is excavated below the first tunnel is less than twice that caused by excavation of the first tunnel.

(2) The convergence of the existing tunnel is more significant when the second tunnel passes below than when it passes above. For the convergence of the tunnel deformation, the maximum convergence position does not occur at the intersection of the crosstunnel space but is offset by a 3D distance from the tunnel intersection.

References

[1]. Liao, S.M., Peng, F. L., & Shen, S. L. (2008). Analysis of shearing effect on tunnel induced by load transfer along longitudinal direction. Journal of Tunnelling and Underground Space Technology, 23(4), 421–430.

[2]. Zhang, Z. X., Liu, C., Huang, X., Kwok, C. Y., & Teng, L. (2016). Three dimensional finite-element analysis on ground responses during twin tunnel construction using the URUP method. Tunnelling and Underground Space Technology, 58, 133–146.

[3]. Do, N. A., Dias, D., Oreste, P., & Djeran-Maigre, I. (2014). The behaviour of the segmental tunnel lining studied by the hyperstatic reaction method. European Journal of Environmental and Civil Engineering, 18(4), 489-510.

[4]. Zhang, Z., & Huang, M. (2014). Geotechnical influence on existing subway tunnels induced by multiline tunneling in Shanghai soft soil. Computers and Geotechnics, 56, 121-132.

[5]. Harris, D. I., Mair, R. J., Love, J. P., Taylor, R. N., & Henderson, T. O.(1994). Observations of ground and structure movements for compensation grouting during tunnel construction at Waterloo station. Geotechnique, 44(4), 691–713.
[6]. Tan, Y., &Wei, B. (2011). Observed behaviors of a long and deep excavation constructed by cut-and-cover technique in Shanghai soft clay. Journal of Geotechnical and Geoenvironmental Engineering, 138(1), 69–88.
[7]. Yang, X. L., & Wang, J. M. (2011). Ground movement prediction for tunnels using simplified procedure. Tunnelling and Underground Space Technology, 26(3), 462-471.
[8]. Divall, S., & Goodey, R. J. (2015). Twin-tunnelling-induced ground movements in clay. Proceedings of the Institution of Civil Engineers-Geotechnical Engineering, 168(3), 247-256.
[9]. Ng, C. W. W., Liu, G. B., & Li, Q. (2013). Investigation of the long-term tunnel settlement mechanisms of the first metro line in Shanghai. Canadian Geotechnical Journal, 50(6), 674–684.
[10]. Jiang, M., & Yin, Z. Y. (2012). Analysis of stress redistribution in soil and earth pressure on tunnel lining using the discrete element method. Tunnelling and Underground Space Technology, 32, 251–259.
[11]. Katebi, H., Rezaei, A. H., Hajialilue-Bonab, M., & Tarifard, A. (2015).Assessment the influence of ground stratification, tunnel and surface buildings specifications on shield tunnel lining loads (by FEM). Tunnelling and Underground Space Technology, 49, 67–78.
[12]. Mo¨ ller, S. C. (2006). Tunnel induced settlements and structural forces in linings. Stuttgart, Germany: Univ. Stuttgart, Inst. f. Geotechnik (pp. 108–125).
[13]. Zhang, Z. X., Liu, C., Huang, X., Kwok, C. Y., & Teng, L. (2016). Three-dimensional finite-element analysis on ground responses during twin-tunnel construction using the URUP method. Tunnelling and Underground Space Technology, 58, 133-146.
[14]. Masın, D., & Herle, I. (2005). Numerical analyses of a tunnel in London clay using different constitutive models. In 5th International symposiumTC28 geotechnical aspects of underground construction in soft ground (Vol. 5, pp. 4–2).
[15]. Shin, J. H., Addenbrooke, T. I., & Potts, D. M. (2002). A numerical study of the effect of groundwater movement on long-term tunnel behaviour. Geotechnique, 52(6), 391-403.
[16]. Standing, J., Potts, D., Vollum, R., Burland, J., Tsiampousi, A., Afshan, S., ... Avgerinos, V. (2015). Investigating the effect of tunnelling on existing tunnels. In Proceedings underground design and construction tunnelling conference, Hong Kong. IOM3, Hong Kong (pp. 310–312).
[17]. Mašın, D., & Herle, I. (2005). Numerical analyses of a tunnel in London clay using different constitutive models. In Proceedings of the 5th international symposium TC28 geotechnical aspects of underground construction in soft ground, Amsterdam, The Netherlands (pp. 595-600).
[18]. Lee, K. M., Rowe, R. K., & Lo, K. Y. (1992). Subsidence owing to tunnelling. I. Estimating the gap parameter. Canadian geotechnical journal, 29(6), 929-940.
[19]. Liu, C., Zhang, Z., & Regueiro, R. A. (2014). Pile and pile group response to tunnelling using a large diameter slurry shield–Case study in Shanghai. Computers and Geotechnics, 59, 21–43.
[20]. Huang, H. W., & Zhang, D. M. (2016). Resilience analysis of shield tunnel lining under extreme surcharge: Characterization and field application. Tunnelling and Underground Space Technology, 51, 301–312.